

On the Flux and Photon Index Distributions of Fermi-LAT Blazars

J. Singal, V. Petrosian, M. Ajello

Stanford / KIPAC / SLAC

We present a determination of the distributions of gamma-ray flux and photon index for the 352 blazars detected at greater than 7σ and above $\pm 20^\circ$ Galactic latitude by the Fermi-LAT in its first year catalog. Our method reconstructs the intrinsic distributions from the observed ones in a way that accounts robustly for the selection biases in the data and correlations among the variables. We find that for the population as a whole the intrinsic flux distribution can be represented by a broken power law of slopes -2.37 ± 0.13 and -1.70 ± 0.26 , and the intrinsic photon index distribution can be represented by a Gaussian with mean 2.41 ± 0.13 and 1σ width of 0.25 ± 0.03 . We also find the intrinsic distributions for the sub populations of BL Lac and FSRQ type blazars considered separately.

Fermi-LAT Blazars

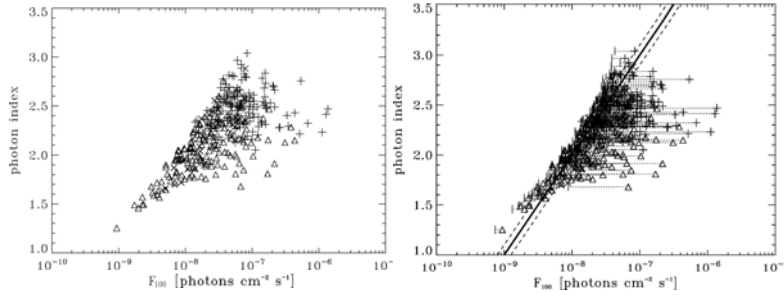


Figure 1: Left: Flux and photon index for the 352 Fermi blazars used in this analysis. BL Lac type blazars ($n=163$) are shown as triangles, FSRQ type blazars ($n=161$) are shown as vertical crosses, and blazars of unidentified or ambiguous type ($n=28$) are represented by Xs. Right: Same, but with the cutoff function shown, along with the approximate limiting flux for each object determined by the detection significance.

We use blazars from the first year Fermi-LAT extragalactic catalog.² Fermi-LAT observations are biased against soft spectrum blazar sources at fluxes below $F_{100} \approx 10^{-7}$ photons $\text{cm}^{-2} \text{sec}^{-1}$. Because of this truncation in the data, and because of the possible inherent correlation between photon index (Γ) and flux (F_{100}), accessing the true distributions of photon index and flux requires care.

Methods

First we determine the correlation between α and F_{100} using the Spearman rank test (SRT) with the method of associated sets,^{3,4} which can deal with truncated data. We approximate the cutoff function with a curve in the Γ, F_{100} plane as discussed in [1]. We then can take out the correlation to form a correlation reduced photon index:

$$\Gamma_{cr} = \Gamma - \beta \cdot \text{Log} \left(\frac{F_{100}}{F_{100-\text{min}}} \right) \quad (1)$$

where β is the best fit correlation parameter. Then the distributions are separable:

$$G(F_{100}, \Gamma) = \psi(F_{100}) \times \hat{h}(\Gamma) \quad (2)$$

and the intrinsic photon index distribution can be recovered by

$$h(\Gamma) = \int_{F_{100}} \psi(F_{100}) \hat{h} \left(\Gamma - \beta \cdot \text{Log} \left(\frac{F_{100}}{F_{100-\text{min}}} \right) \right) dF_{100} \quad (3)$$

Distributions

We form the distributions $\psi(F_{100})$ and $\hat{h}(\Gamma)$ using the Lynden-Bell method modified with associated sets^{3,4} to account for the truncation in the Γ, F_{100} plane. A full discussion is provided in [1].

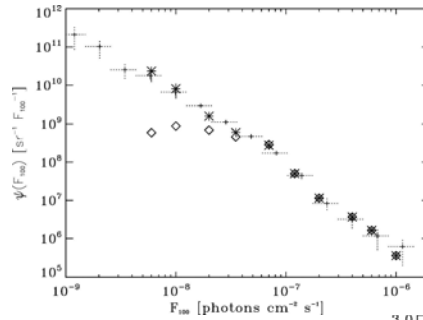


Figure 2: Observed (diamonds) and reconstructed intrinsic (stars) distribution of flux $\psi(F_{100})$ for the 352 Fermi blazars used in this analysis. We also plot $\psi(F_{100})$ as determined in MA⁵ (small crosses), with error bars (dotted lines).

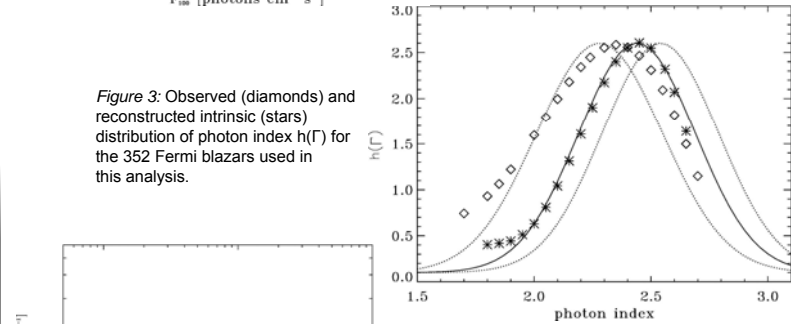


Figure 3: Observed (diamonds) and reconstructed intrinsic (stars) distribution of photon index $h(\Gamma)$ for the 352 Fermi blazars used in this analysis.

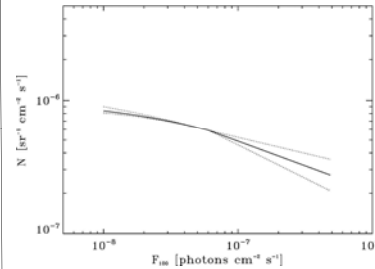


Figure 4: Estimate of the total cumulative photon density from blazars. The diffuse gamma-ray background would correspond to $\sim 1 \times 10^{-5} \text{ cm}^{-2} \text{ sec}^{-1} \text{ sr}^{-1}$ in these units.⁶

	n	β^a	m_{above}^b	F_{break}^c	m_{below}^d	μ^e	σ^f
Blazars ^g (this work)	352	0.02 ± 0.08	-2.37 ± 0.13	6.0	-1.70 ± 0.26	2.41 ± 0.13	0.25 ± 0.03
Blazars ^g (MA) ⁵	352	-	-2.48 ± 0.13	7.39 ± 1.01	-1.57 ± 0.09	2.37 ± 0.02	0.28 ± 0.01
BL Lacs (this work)	163	0.04 ± 0.09	-2.55 ± 0.17	5.5	-1.61 ± 0.27	2.13 ± 0.13	0.24 ± 0.02
BL Lacs (MA) ⁵	163	-	-2.74 ± 0.30	6.77 ± 1.30	-1.72 ± 0.14	2.18 ± 0.02	0.23 ± 0.01
FSRQs (this work)	161	-0.11 ± 0.06	-2.22 ± 0.09	6.0	-1.62 ± 0.55	2.52 ± 0.08	0.17 ± 0.02
FSRQs (MA) ⁵	161	-	-2.41 ± 0.16	6.12 ± 1.30	-0.70 ± 0.30	2.48 ± 0.02	0.18 ± 0.01

^a The correlation between photon index Γ and flux F_{100} . See Equation 1 and §3.1.

^b The slope of the intrinsic flux distribution $\psi(F_{100})$ at fluxes above the break.

^c The flux at which the power law break in $\psi(F_{100})$ occurs, in units of 10^{-8} photons $\text{cm}^{-2} \text{sec}^{-1}$. In MA this is a fit, while in this work it is a visual inspection, as precise location of the break is not important for this analysis.

^d The slope of the intrinsic flux distribution $\psi(F_{100})$ at fluxes below the break.

^e The mean of the Gaussian fit to the intrinsic photon index distribution $h(\Gamma)$. For the analysis here this includes the full range of results and their uncertainties when considering the 1σ range of β .

^f The 1σ width of the Gaussian fit to the intrinsic photon index distribution $h(\Gamma)$.

^g Including all FSRQs, BL Lacs, and 28 of unidentified type.

References: ¹J. Singal, V. Petrosian, & M. Ajello, 2011, *in prep*

²A. Abdo et al. 2010, *ApJ*, 715, 429; ³B. Efron, & V. Petrosian, 1992, *ApJ*, 399, 345;

⁴V. Petrosian, 1992, in *Statistical Challenges in Modern Astronomy*, 173;

⁵Abdo, A., et al. 2010, *ApJ*, 720, 435 ("MA"), ⁶Abdo, A., et al. 2010, *PhysRevLett*, 104, 101101